SOME PRACTICAL CONSEQUENCES OF ANALYSES OF THE CARBOXY AND AIRBURN REACTIONS OF ANODE CARBONS

N. Bird, B. McEnaney* and B. A. Sadler
Comalco Research Centre, Thomastown, Victoria 3074, Australia
*School of Materials Science, University of Bath, Bath BA2 7AY, UK

Abstract

An analysis of the carboxy reaction shows that the reaction rate is controlled by the chemical reactivity of the carbon and in-pore diffusion. An analysis of the airburn reaction shows that the rate at high temperatures is controlled by boundary layer diffusion and at low temperatures by boundary layer diffusion and in-pore diffusion. For the carboxy reaction the analysis enables benefits from optimising green mix formulation, final heat treatment temperature, etc., to be assessed. The airburn reaction is much less sensitive to carbon structure and reactivity. The analysis adapted to model the effect of cover is able to predict the reduction in the airburn rate with increasing depth of cover.

Introduction

Airburn and carboxy reactions of anodes account for significant proportions of anode consumption. Grjotheim and Welch (1) report that airburn contributes from 8 to 20 % and carboxy reaction contributes from 4 to 8 % of theoretical carbon consumption. In both types of reaction the overall rate may be influenced by the intrinsic reactivity of the anode carbon and the transport of reactant and product gases to and from reaction sites. The importance of gaseous diffusion in both types of gas-anode carbon reaction has been recognised by many workers (e.g., 2,3) but there are not many detailed theoretical studies of diffusion and reaction in anode carbons. The development of more quantitative treatments of the reaction of gases with anode carbons will lead to improvements in understanding the role of these reactions in the consumption of anodes in service and the development of realistic strategies for ameliorating these problems. It may also provide improved reactivity parameters for input to computer models of anodes in service which are being developed in the industry.

Arrhenius plots for gas-carbon reactions are often curved with the apparent activation energy, E_a, decreasing with increasing temperature. An idealised plot, Fig. 1, shows three zones: I, II, and III. and two transitional regions: a, b. In general there are three resistances affecting the overall rate of gasification of carbons: (i) the resistance due to the intrinsic chemical reactivity of the carbon surface, which is dominant at low temperatures in Zone I; (ii) the resistance due to in-pore diffusion (dominant in Zone II); (iii) the resistance due to boundary layer diffusion (dominant at high temperatures in Zone III). In the transitional regions a and b the adjacent resistances are of comparable magnitude.

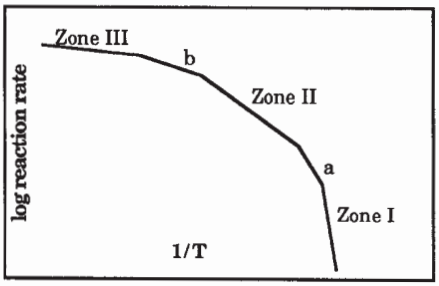

Figure 1. Schematic Arrhenius plot for gas-carbon reactions

There are three parts to this paper (i) an experimental study and analysis of the role of in-pore diffusion on the carboxy reaction using the standard carboxy reactivity apparatus (4); (ii) an analysis of the airburn reaction rate and the effects of cover using previously published data, and (iii) consideration of some practical implications of the analyses.

The Carboxy Reaction

Experimental

Cylindrical cores, 60mm length, 45mm diameter, were drilled from a pre-baked anode, apparent density = 1.52 g/ml. Duplicate samples were oxidised under standard conditions (4):- 960 °C for 7 h in flowing CO_2, flow rate = 200 l/h at 2 bar. Samples were also oxidised at 900 and 1000 °C with the other experimental conditions unchanged. Oxidation rates were calculated from the

A. Tomsett and J. Johnson (Eds.), *Essential Readings in Light Metals*

weight change of the specimens after gasification. Because the carboxy reaction is inhibited by the product CO, the CO content of the gas in the furnace was measured using an infra-red detector and a sampling probe held at 5 and 50 mm above the carbon sample. Changes in pore size distribution following gasification of the anode cores were also measured using mercury porosimetry.

Results

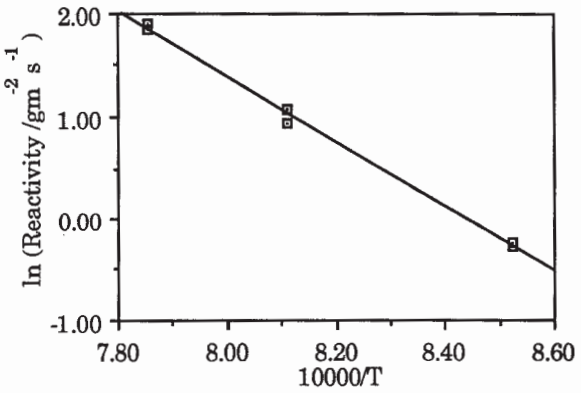

Figure 2. Arrhenius plot for the carboxy reactivity of anode carbons.

Fig. 2 shows the reaction rates as an Arrhenius plot giving an apparent activation energy, E_a = 265 kJ/mol. At 960 °C the CO content of the gas in the furnace increased from 0.5% to 1.5% during the course of a 7 h experiment; there was very little difference in CO content at 5 and 50 mm above the sample. Mercury porosimetry showed that after gasification there was development of porosity through to the centre of the samples. This is illustrated in Fig. 3 which compares the pore size distributions from the centre of a sample after gasification and that from an unreacted carbon.

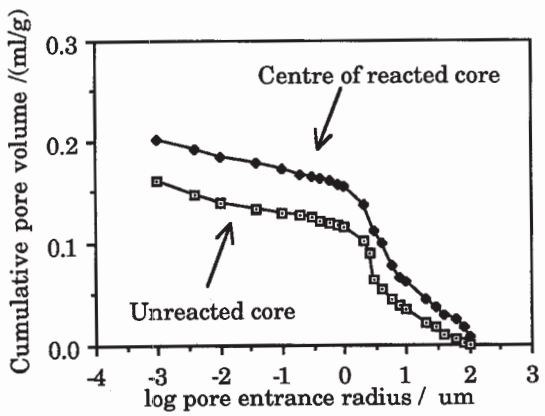

Figure 3. Pore size distributions for anode carbons before and after gasification.

Discussion.

Fig. 3 shows clearly that the carboxy reaction occurs within the pores of the carbon through to the centre of the sample so that both chemical factors and in-pore diffusion may be influencing the rate. A model for the C-CO_2 reaction occurring in the Zone I - Zone II regions developed by Stephen and McEnaney (5) takes account of inhibition by CO and Stefan flow due to the outwardly-diffusing CO. Details of the analysis have been published (6). It was concluded that in the laboratory experiments the carboxy reaction occurs in transitional Zone a, but close to Zone II. A sketch of the CO_2 concentration profile is in Fig 4a. This analysis is in good accord with the experimental results, since Fig. 3 shows that the reactant gas penetrates to the centre of the anode core, as expected in Zone a conditions. Similar changes in pore size distributions have been observed in samples cut from behind the electrolytic face of anode carbons after service (7). However, these isothermal, isobaric laboratory experiments differ from operating conditions, where the carboxy reaction occurs under a thermal gradient and a small pressure gradient.

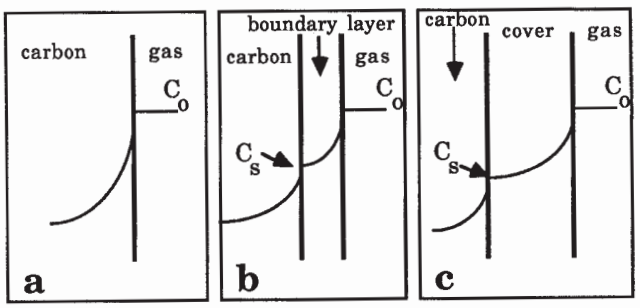

Figure 4. Reactant gas concentration profiles: **a.** CO_2 in carboxy reaction; **b.** O_2 in airburn reaction in Zone b; C_s = 0 in Zone III; **c.** effect of cover on O_2 profile in airburn reaction.

The Airburn Reaction.

Introduction

The intrinsic reaction mechanism of the C-O_2 reaction is complex and not well-understood. One reason is that the reaction is subject to instabilities associated with its exothermicity so that many published kinetic studies were not carried out under truly isothermal conditions (8). Another uncertainty is the exact composition of the primary product gases; both CO and CO_2 can be produced and the secondary reaction

$$2CO + O_2 = 2CO_2$$

can occur in the gas phase. There appear to have been no studies of the reaction order for airburn of anodes nor has the CO/CO_2 ratio been measured or the combustion behaviour been studied in any detail.

Results

Some useful data for airburn of anodes were obtained by Hannah (9) The Arrhenius plot, Fig. 5, shows pronounced curvature indicative of mass transport effects influencing the rate. The value of E_a in the temperature range 580-620 °C is 15 kJ/mol, indicative of boundary layer effects influencing the rate. In the temperature range 400-470 °C the value of E_a is 235 kJ/mol. Laurendau (10) has proposed that the activation energy in Zone I = 290-335 kJ/mol for the C-O_2 reaction at T< ~730 °C, suggesting that in-pore diffusion contributes to the rate of oxidation of the anode carbon in this temperature range.

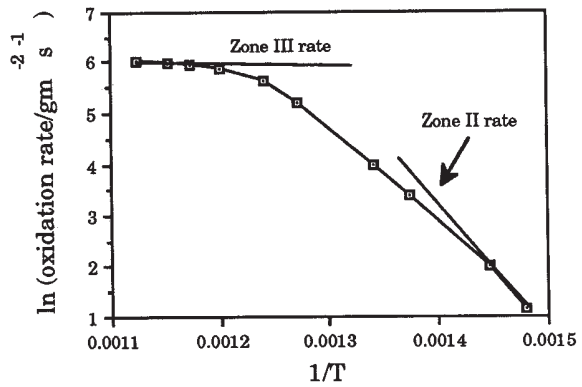

Figure 5 Arrhenius plot for the airburn reaction; data from (9). Zone II and III rates calculated from Equn. (3).

Analysis

If it is assumed that the sole product of the C-O_2 reaction is CO_2, so that Stefan flow due to the production of CO can be neglected, then, assuming stagnant conditions, the reaction rate in Zone III, R_e, is

$$R_e = \Lambda D C_0 / \delta = K_{III} C_0, \qquad (1)$$

where D is the free-gas difusivity of O_2 in the boundary layer of width δ, K_{III} is the mass transfer coefficient in Zone III and Λ is a stoichiometric coefficient. From kinetic theory, $D \alpha T^{1.85}$, $C_0 \alpha T^{-1}$, and thus $R_e \alpha T^{0.85}$, assuming δ is independent of temperature. The ratios $[R_e(T) / R_e(890\ K)]$ and $[T / 890]^{0.85}$ for the data in Fig.5 over the range 806-890 K are compared in Table I, which shows that between 867 and 890 K (594-617 °C) the overall rate increase is very close to that predicted by $R_e \alpha T^{0.85}$. At lower temperatures, the rate is less than predicted, indicating that chemical factors and in-pore diffusion are influencing the rate.

Table I Test for Zone III conditions for data in Fig. 5

Temp / K	$R_e(T) / R_e(890\ K)$	$(T / 890)^{0.85}$
867	0.976	0.978
853	0.915	0.965
833	0.863	0.945
806	0.727	0.919

In the transitional zone b, where the resistances due to boundary layer diffusion and in-pore diffusion are of comparable magnitude, the O_2 concentration profile is as in Fig 4b. Assuming steady state conditions, the mass balance at the external surface of the carbon requires that

$$R_e = K_{III} (C_0 - C_s) = K_{II} C_s, \qquad (2)$$

where C_s is the surface concentration of O_2 and K_{II} is the mass transfer coefficient in the pores of the carbon. Eliminating C_s in Equn. (2) gives

$$R_e = C_0 (1 / K_{II} - 1 / K_{III})^{-1}. \qquad (3)$$

If it assumed that the overall rate at 890 K represents the Zone III rate, then the value of K_{III} at that temperature can be calculated. If it is further assumed that the temperature coefficient of K_{III} is dominated by that of D, then the value of K_{III} at each temperature can be calculated from

$$K_{III}(T) = [K_{III} (890\ K)] (T / 890)^{1.85}. \qquad (4)$$

The computed Zone III and Zone II reaction rates are compared to the experimental reaction rates in Fig 5, which shows that the Zone II - Zone b transition occurs at about 450 °C and the Zone b - Zone III transition at about 570 °C, in good agreement with the qualitative interpretion presented in the "Results" section.

Practical Implications

The Carboxy Reaction

The kinetic analysis presented above shows that the carboxy reaction occurs in the transitional zone a, close to Zone II. In Zone II

$$R_e \alpha (k_1 D_e)^{1/2}, \qquad (5)$$

where k_1 is a C-CO_2 reaction rate constant and D_e is the effective diffusivity of CO_2 in the pores of the carbon. D_e

is directly proportional to the open pore volume fraction, P, (11):

$$D_e / D = P / 2 \qquad (6)$$

and k_1 is directly proportional to the active surface area of the anode carbon, A_a, so that

$$R_e \alpha (A_a P)^{1/2} . \qquad (7)$$

This proportionality allows reductions in anode consumption rate due to the carboxy reaction following changes in P and A_a to be estimated. For example, increasing the final baking temperature will lead to a decrease in A_a without changing P significantly. The presence of catalytic impurities in the anode will increase A_a without affecting P significantly. Variations in green mix formulations designed to reduce P may also reduce A_a, producing a double benefit. Work is in hand to test the validity of these arguments by making independent estimates of A_a and P for anode carbons subject to different final baking temperatures. In practice, the effects of varying P and A_a on the carboxy reaction rate may be small, both because of the square root relationship between R_e and the product (A_aP) Equn. (7), and the limited scope for varying these parameters in anode fabrication technology.

The Airburn Reaction

The rate of the airburn reaction is dominated by mass transfer effects at the boundary layer, particularly at high temperatures. Thus the airburn rate is much less sensitive to the structure and reactivity of the anode than is the carboxy reaction. Increasing the final baking temperature of the anode will increase its thermal conductivity, and hence the temperature of the surface of the anode exposed to the atmosphere. In practice, temperature increases up to 200 °C have been recorded on anodes. According to this analysis, the increase in the airburn rate should be modest if the reaction occurs in Zone III. For example, a temperature increase from 450 to 650 °C would result in an increase in R_e of 23%, assuming $R_e \alpha T^{0.85}$. For the moment this analysis should be treated with caution, since it takes no account of the instabilities of the airburn reaction, due to its exothermicity, which can give rise to sudden increases in temperature in the airburn reaction zone.

Effect of cover upon the airburn reaction.

It is possible to model the influence of cover on the airburn rate, if it is assumed that the rate of reaction is controlled by a combination of gaseous diffusion through the cover and diffusion and reaction within the pores of the anode carbon; a sketch of the O_2 concentration profile is in Fig. 4c. Assuming steady state gasification and stagnant gas conditions,

$$R_e = \Lambda D_e' (C_o - C_s) / d = K_{II} C_s \qquad (8)$$

where D_e' is the effective diffusivity of oxygen through the cover of thickness d. Fitchett et al (12,13) have shown that reactivity of anode carbons decreases progressively with depth of cover. Some of their data for carbons of a range of quality are in Fig. 6. The steady state rate of airburn depends upon the concentration of oxygen at the carbon surface, C_s. Qualitatively, the progressive reduction in airburn rate with increasing depth of cover can be attributed to a decrease in C_s, Fig 4c. At large d, $C_o >> C_s$ and Equn. (8) reduces to

$$R_e = \Lambda D_e' C_o / d. \qquad (9)$$

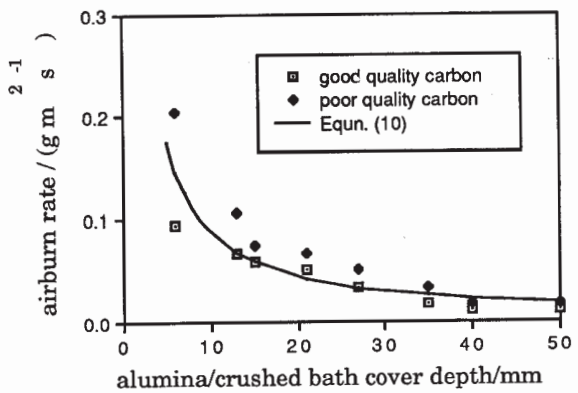

Figure 6 Effect of alumina/crushed bath cover depth on oxidation rate; data from (13); line calculated from Equn. (10).

The experimental data in Fig. 6 show that the airburn rate becomes independent of carbon quality and therefore, presumably, dominated by diffusion through the cover for values of d > ~30 mm. If Equn. (9) is assumed to be valid for d > 30 mm, its ability to predict R_e(i) at other cover depths, d(i), can be tested by

$$R_e(i) = R_e(1)\, d(1) / d(i) \qquad (10)$$

where R_e(1) is the gasification rate for cover of depth d(1) > 30 mm. The resulting curve in Fig. 6, using d(1) = 35 mm and the mean value of R_e(1), shows that Equn (10) provides a reasonable prediction of the effects of depth of cover on airburn rates.

The practical implication of this analysis is that the effectiveness of anode cover depends upon minimising the open pore volume, e.g., by varying its granulometry, as demonstrated by Fitchett et al (12,13). Provided the

cover is deep enough for Equn. (9) to be valid, it is expected that the airburn rate will be reduced in direct proportion to the reduction in open pore volume. It will be interesting to further test these predictions by relating reductions in airburn rate to direct measurements of P and D_e' for different types and depths of cover.

Acknowledgement

We thank G Kaiser of Comalco Research Centre, Australia, for useful comments.

Notation

A_a	active surface area (m^2g^{-1})
C_o; C_s	reactant gas concentration: in bulk; at external surface of carbon ($g\ m^{-3}$)
D	diffusivity of reactant gas (m^2s^{-1})
D_e; D_e'	effective diffusivity of reactant gas: in pores of carbon; in cover (m^2s^{-1})
d	depth of cover (m)
E_a	apparent activation energy ($kJ\ mol^{-1}$)
K_{II}; K_{III}	mass transfer coefficients: in pores of carbon; in boundary layer ($m\ s^{-1}$)
k_1	C-CO_2 reaction rate constant
P	open pore volume fraction.
R_e	reaction rate ($gm^{-2}s^{-1}$)
δ	boundary layer thickness (m)
Λ	gravimetric stoichiometric coefficient

References.

1. K. Grjotheim and B.J. Welch, Aluminium Smelter Technology, 2nd Ed., (Aluminium Verlag, Dusseldorf FRG, 1988) p. 155.

2. T. Foosnaes and T. Naterstad, In, Understanding the Hall-Heroult Process for the Production of Aluminium, Ed. K. Grjotheim and H. Kvande (Aluminium Verlag, Dusseldorf FRG, 1986) p. 97.

3. J.F. Rey Boero, In Light Metals, 1983, (Metallurgical Soc., of AIME, Warrendale, PA, USA, 1983) 867-884.

4. W.K. Fischer and R. Perrochoud, J Metals, (November 1987) 43-45.

5. W.J. Stephen and B. McEnaney, Proc. 5th London Conference on Industrial Carbon and Graphite, (Soc. Chem. Ind., London, UK, 1978) 97-107.

6. N. Bird, B McEnaney and B A Sadler, Extended Abstracts, 19th American Carbon Conference, Pennsylvania State University, June 1989 (American Carbon Society, 1989) 568-569.

7. B.A. Sadler, Comalco Research Centre, Thomastown Australia, unpublished results.

8. J.F. Rey Boero, Carbon, 20, (1982), 535-536.

9. R.C. Hannah, Comalco Aluminium (Bell Bay) Ltd., Australia, Report No 150 (1981) 1-24.

10. N.M. Laurendau, Prog. Energy Combust. Sci., 4, (1978) 221-270.

11. C.N. Satterfield, Mass Transfer in Heterogeneous Catalysis, (MIT Press, Cambridge, MA, USA, 1970)

12. A.M. Fitchett, D.J. Morgan, and B.J. Welch, Light Metals 1988 Ed.L G Boxall (Metallurgical Soc. of AIME, Warrendale, PA, USA, 1988) 291-294.

13. A.M. Fitchett, The Oxidation and Protection of Heterogeneous Carbon Anodes used for Aluminium Smelting, (Ph.D Thesis, 1988, University of Auckland, NZ.) 92-124.